BIOCHEMISTRY
including biophysical chemistry & molecular biology
Article

Biochemistry **2009,** *48,* 7399–7410 7399
DOI: 10.1021/bi9008006

Escherichia coli DNA Adenine Methyltransferase: Intrasite Processivity and Substrate-Induced Dimerization and Activation

Stephanie R. Coffin and Norbert O. Reich*

Department of Chemistry and Biochemistry and Biomolecular Science and Engineering Program, University of California, Santa Barbara, California 93106-9510

Received May 9, 2009; Revised Manuscript Received June 30, 2009

ABSTRACT: Methylation of GATC sites in *Escherichia coli* by DNA adenine methyltransferase (EcoDam) is essential for proper DNA replication timing, gene regulation, and mismatch repair. The low cellular concentration of EcoDam and the high number of GATC sites in the genome (~20000) support the reliance on methylation efficiency-enhancing strategies such as extensive intersite processivity. Here, we present evidence that EcoDam has evolved other unique mechanisms of activation not commonly observed with restriction−modification methyltransferases. EcoDam dimerizes on short, synthetic DNA, resulting in enhanced catalysis; however, dimerization is not observed on large genomic DNA where the potential for intersite processive methylation precludes any dimerization-dependent activation. An activated form of the enzyme is apparent on large genomic DNA and can also be achieved with high concentrations of short, synthetic substrates. We suggest that this activation is inherent on polymeric DNA where either multiple GATC sites are available for methylation or the partitioning of the enzyme onto nonspecific DNA is favored. Unlike other restriction−modification methyltransferases, EcoDam carries out intrasite processive catalysis whereby the enzyme−DNA complex methylates both strands of an unmethylated GATC site prior to dissociation from the DNA. This occurs with short 21 bp oligonucleotides and is highly dependent upon salt concentrations. Kinetic modeling which invokes enzyme activation by both dimerization and excess substrate provides mechanistic insights into key regulatory checkpoints for an enzyme involved in multiple, diverse biological pathways.

Bacterial DNA methyltransferases catalyze the *S*-adenosylmethionine-dependent methylation of cytosines at the C-5 or N-4 position or adenines at the N-6 position (*1*, *2*). Most bacterial methyltransferases, like the well-characterized C-5 methyltransferase M.HhaI, are involved in restriction modification systems which serve to protect the cell from invading DNA (*3*, *4*). Others, like the orphan methyltransferase *Escherichia coli* DNA adenine methyltransferase (EcoDam)[1] and the cell cycle-regulated methyltransferase in *Caulobacter crescentus* (CcrM), do not participate in such a system. Instead, these enzymes are involved in diverse biological pathways such as gene regulation, mismatch repair, DNA replication, and nucleoid structure determination and are not partnered with a cognate restriction endonuclease (*5*−*8*). While CcrM homologous are widespread in α-proteobacteria (*9*), EcoDam homologues are found in many γ-proteobacteria such as *Salmonella typhimurium* (*10*), *Yersinia pseudotuberculosis* (*11*), *Vibrio cholerae* (*11*), *Actinobacillus actinomycetemcomitans* (*12*), and *Haemophilus influenzae* (*13*). A growing number of these bacterial pathogens require methylation for virulence (*14*), and gene expression and proteomic studies of bacteria in which the EcoDam gene has been deleted show dramatic and widespread changes in RNA and protein levels, in many cases involving well-characterized virulence factors (*15*−*18*). These findings have implicated EcoDam and CcrM as antibiotic targets for combatting the ever-increasing number of antibiotic resistant bacteria (*19*), and current inhibition efforts are being made in this regard (*20*).

EcoDam belongs to the α-class of adenine methyltransferases and transfers a methyl group to the N-6 position of the adenine in the DNA sequence 5′-GATC-3′ (*21*). EcoDam methylates multiple GATC sites in a highly processive manner, catalyzing multiple methylation events prior to dissociating from the DNA (*22*). Processivity is essential for methylation of the ~20000 GATC sites within the *E. coli* genome and the relatively few EcoDam molecules present in the cell (*23*, *24*). The lack of methylation of GATC sites within the *E. coli* genome results in hypermutation of phenotypes most likely due to its role in signaling the mismatch repair machinery (*25*, *27*). Because the most biologically prevalent substrate for bacterial methyltransferases is hemimethylated DNA where only one methyl group is transferred per cognate site, it is understandable that methyltransferases are typically active monomers. However, many methyltransferases (*28*), including T4 Dam (*29*) and M.DpnII (*30*) from the α-class of adenine methyltransferases, dimerize in solution. In the case of T4 Dam, this observed dimerization is substrate-dependent (*31*). Many of the β-class methyltransferases such as CcrM (*32*), M.LlaCI (*33*), and M.KpnI (*34*) have also been

*Ro whom correspondence should be addressed. E-mail: reich@chem.ucsb.edu. Phone: (805) 893-8368. Fax: (805) 893-4120.

[1]Abbreviations: EcoDam, *E. coli* DNA adenine methyltransferase; IPTG, isopropyl 1-thio-β-D-galactopyranoside; BSA, bovine serum albumin; DTT, dithiothreitol; AdoMet, *S*-adenosylmethionine; CcrM, cell cycle-regulated methyltransferase in *C. crescentus*; Lrp, leucine response protein; PAGE, polyacrylamide gel electrophoresis; MRB, methylation reaction buffer; WT, wild type; SDS, sodium dodecyl sulfate; MSC, Model Selection Criterion; AIC, Akaike Information Criterion.

Published on Web 07/06/2009

shown to dimerize in solution. Further, two methyltransferases in this class, MboIIA (*35*) and M.RsrI (*36*), have been crystallized in their dimeric state. It has been suggested that dimerization of DNA-modifying enzymes could create a large enzyme−substrate network with high-molecular weight DNA (*37*). This larger interface with the DNA would enhance processive catalysis and facilitated diffusion, thus rendering the enzyme more active on large DNA where continued association to the substrate is easily achieved. Although EcoDam has not been shown to be dimeric, responsiveness to high-molecular weight DNA on activity has certainly been observed and is consistent with computer simulation efforts (*22*).

The involvement of EcoDam in such diverse biological pathways suggests that the enzyme may rely on regulatory mechanisms that go beyond the efficient methylation of GATC sites. For example, we recently demonstrated that under certain conditions, EcoDam and the leucine response protein (Lrp) compete to regulate *pap* expression which encodes pilus proteins necessary for uropathogenic *E. coli* cellular adhesion (*38*). Prior to this work, it was assumed that the presence of Lrp alone detoured EcoDam methylation, thus rendering the enzyme inactive on the epigenetically regulated gene. However, Dam actively competes with Lrp for GATC sites, with the actual binding preference determined by the sequence context. Similarly, the regulatory protein OxyR and EcoDam compete for three GATC sites located in the *agn43* operon important for biofilm production (*39*). The regulation of EcoDam and the lack of methylation of GATC sites in the 5′ noncoding regions of genes (*40*, *41*) may go beyond the kinetic and thermodynamic competition with other proteins, such as the nature of the DNA surrounding its cognate site (*42*, *43*). Similarly, EcoDam has been shown to bind its cofactor in two orientations via NMR (*44*) and crystallography (*45*) which, although not functionally characterized, may be the basis of an additional, novel, pathway-specific form of regulation.

The processive methylation and higher-order specificity characteristics of EcoDam are in part modulated by the DNA surrounding its cognate site (*42*, *43*). On the basis of these observations, we predicted that EcoDam has evolved a highly conserved enzyme−DNA interface that facilitates both processive catalysis and higher-order specificity. This prediction was recently validated by mutagenic analysis of the conserved enzyme−DNA interface (*46*). Here we present evidence that the highly evolved enzyme−DNA interface of EcoDam is also responsible for unique kinetic activity distinct from that of other restriction modification methyltransferases. We observe substrate-induced dimeric activity that requires an intact native enzyme−DNA interface (*46*) that is not observed with large genomic DNA. Additionally, we demonstrate that EcoDam utilizes two forms of processive catalysis: intersite processivity whereby multiple GATC sites on the same DNA molecule are methylated and intrasite processivity where the monomeric enzyme methylates both strands of a single unmethylated duplex prior to dissociating from the substrate. We suggest that our observations offer insight into the different means by which EcoDam has evolved to satisfy the diverse number pathways in which it is involved.

EXPERIMENTAL PROCEDURES

Enzyme Expression and Purification. EcoDam was expressed and purified as previously described (*42*). In brief, EcoDam was overexpressed in XL2-Blue (Stratagene) *E. coli* cells grown at 37 °C in LB medium supplemented with 25 μg/mL kanamycin and 12.5 μg/mL tetracycline. Once an OD_{600} of 0.4−0.6 was reached, cells were induced with 1 mM IPTG and 0.05% L-arabinose and grown for 2 h at 37 °C. Pelleted cells were resuspended in 40−60 mL of P-11 buffer [50 mM potassium phosphate buffer (pH 7.4), 10 mM β-mercaptoethanol, 1 mM EDTA, 1 mM phenylmethanesulfonyl fluoride, 0.2 M NaCl, and 10% glycerol] and lysed with a French press. The lysate was centrifuged at 15000 rpm for 60 min at 4 °C and the supernatant loaded unto a 60 mL phosphocellulose (Whatman) column. The protein was eluted with a salt gradient between 0.2 and 0.8 M NaCl, and those fractions containing EcoDam were pooled and dialyzed in BS buffer [20 mM potassium phosphate buffer (pH 7.0), 10 mM β-mercaptoethanol, 1 mM EDTA, 1 mM phenylmethanesulfonyl fluoride, and 10% glycerol]. The dialyzed protein was loaded onto a 20 mL Blue Sepharose 6 Fast Flow (GE Healthcare) column pre-equilibrated in BS buffer and protein eluted with a salt gradient between 0 and 1.5 M NaCl. Fractions containing EcoDam were flash-frozen and stored at −80 °C. Concentrations were determined using an extinction coefficient of 1.16 mL mg^{-1} cm^{-1} at 280 nm.

DNA Substrates. All DNA oligonucleotides were ordered from Operon and resuspended in TE [10 mM Tris (pH 7.5) and 1 mM EDTA]. All constructs were annealed in a 1:1 molar ratio by being heated at 95 °C for 10 min and then slowly cooled (∼5 h) to 22 °C. Proper product formation was verified by PAGE. The preferred substrate (P) consisted of the annealed product of oligonucleotides 5′-CATTTACTTGATCCGGTATGC-3′ and 5′-GCATACCGGATCAAGTAAATG-3′, while the nonpreferred substrate (N-P) consisted of the annealed product of oligonucleotides 5′-CATTTAGACGATCTTTTATGC-3′ and 5′-GCATAAAAGATCGTCTAAATG-3′. Concentrations of all DNA constructs were determined by measuring the A_{260}. Calf thymus DNA was ordered from Sigma-Aldrich. DNA labeled with a 5′ terminal fluorescein for use in anisotropy experiments was ordered HPLC purified from Midland and processed as described above.

K_D^{DNA} Determination. Anisotropy experiments were performed on a Fluoromax-2 fluorimeter (ISA SPEX) equipped with an L-format autopolarizer at 22 °C. The change in anisotropy of 20 nM singly labeled (fluorescein) duplex DNA in MRB [100 mM Tris (pH 8.0), 1 mM EDTA, 1 mM DTT, and 0.2 mg/mL BSA] supplemented with 50 μM sinefungin was monitored as an increasing amount of enzyme was added. Data for each addition of enzyme were collected by monitoring the excitation at 494 nm and emission at 518 nm. Slit widths of 8 nm were used for all experiments. The resultant changes in anisotropy were plotted against enzyme concentration, and the dissociation constant was derived by fitting the data to the modified quadratic equation:

$$f = \frac{a+x+b-[(a+x+b)^2-4xa]^{1/2}}{2}$$

where $b = K_D$, x = [enzyme][DNA], and a = [enzyme−DNA]. An additional graphical analysis was completed by also fitting the data to the Hill equation:

$$f = \frac{ax^b}{c^b+x^b}$$

where b is equal to the Hill coefficient. All graphical analysis was done with Sigma Plot 6.1 (SSPS, Inc.).

Stoichiometric Titration. A gel mobility shift assay was performed on the 21 bp fluorescein-labeled DNA used for anisotropy experiments. Binding reactions took place in MRB in the presence of a saturating level of sinefungin (50 μM). In this case, the DNA (500 nM) was retained at a concentration in 5-fold molar excess in relation to the calculated K_D^{DNA}. EcoDam was titrated below and above the concentration of DNA, and the results were visualized via 15% nondenaturing PAGE. Gels were scanned on a Storm 840 PhosphorImager (Amersham Biosciences). Band density was determined using Image-Quant version 1.2 (Molecular Dynamics Inc.) and further analyzed in Microsoft Excel. The loss of density in the DNA band was plotted versus enzyme concentration in Sigma Plot 6.1. Under these conditions, a linear dependence on binding was observed until stoichiometric saturation was reached. The concentration of enzyme at which this linear dependency stops is equal to the concentration of enzyme (1000 nM) required to saturate the substrate (500 nM). The molar ratio of the two concentrations at this point is 2:1, indicating the ability of two EcoDam molecules to bind to one DNA strand.

Steady State Assays. Incorporation of tritiated methyl groups onto DNA was monitored by a filter binding assay as previously described (*47*). EcoDam was diluted in protein dilution buffer [20 mM potassium phosphate (pH 7.5), 200 mM NaCl, 0.2 mM EDTA, 0.2 mg/mL BSA, 2 mM DTT, and 10% glycerol]. Reactions were conducted at 22 °C, and mixtures contained 2 nM EcoDam in MRB, 0.2 mg/mL BSA, 25 μM AdoMet, and 21 bp DNA (0−10000 nM) in a final volume of 20 μL. Mixtures were allowed to equilibrate at 22 °C prior to initiation of the reaction with DNA. For calf thymus DNA experiments, DNA was reported in concentrations of base pairs and equilibrated to the concentrations of the 21 bp oligo. Reactions were quenched with 10 μL of 1% SDS at a single time point (30 min), and 25 μL was spotted onto 2.5 cm Whatman DE81 circular filter papers. Additional steady state experiments with increasing enzyme concentrations (10 and 50 nM) were performed with decreased reaction times (7 and 0.5 min). Filter papers were washed three times in 50 mM KH_2PO_4, once in 80% ethanol, once in 100% ethanol, and once in diethyl ether for 5 min each. Papers were dried and submerged in BioSafeII scintillation fluid. Tritium levels were quantitated in a Beckman-Coulter LS6500 scintillation counter. Counts were converted to methylated product per unit time and plotted against the DNA concentration. Values for K_M^{DNA} and k_{cat} were found by fitting the data to a rectangular hyperbola in Sigma Plot 6.1.

Burst Analysis. Reactions were conducted in MRB with 50 nM enzyme, 500 nM DNA, and 30 μM tritiated AdoMet at 22 °C. Reactions were quenched by placing 10 μL aliquots of the reaction mixture into an equal volume of 1% SDS at time points of 0, 15, 30, 45, 60, 90, and 120 s. Fifteen microliters of the resulting mixture was spotted on DE81 filter papers and washed as described above. Tritium levels were quantitated, converted to methylated product, and plotted versus time in Sigma Plot. The k_{cat}^{app} (not shown) was found by fitting the data to a linear curve and dividing the slope of the line by the enzyme concentration. This value was comparable to the actual k_{cat} of WT and mutant enzymes. The *y*-intercept of the linear fit to the data represents the burst magnitude.

Single-Turnover Assays. The incorporation of methyl groups under single-turnover conditions was monitored at 4 °C with DNA limiting and EcoDam and AdoMet in excess. Reactions took place in MRB with 0.2 mg/mL BSA, 400 nM DNA, 420 nM EcoDam, and 30 μM AdoMet in a total volume of 100 μL. All reactions were initiated with addition of DNA. At 0, 10, 20, 30, 45, 60, 120, and 180 s, 10 μL aliquots of the reaction mixture were removed and quenched in 10 μL of 1% SDS. Fifteen microliters of the resulting mixture was spotted on DE81 filter paper. Samples were washed, dried, and counted as described above. Counts were converted to nanomolar methylated product and plotted versus time. The k_{chem} for each substrate was found by fitting the data to a single exponential in Sigma Plot 6.1. For salt dependency assays, the same protocol was followed except the DNA concentration was 300 nM and the enzyme concentration was 320 nM while the NaCl concentration varied between 50 and 450 mM in MRB. The resulting asymptote as derived at a single time point (120 s) was plotted versus salt concentration, and the results were fit to a four-parameter logistic curve in Sigma Plot.

Initial Velocity Studies. The initial velocity of WT EcoDam was monitored at various enzyme concentrations at time points that were within the early phase of product formation (< 35% conversion). Reaction mixtures contained various concentrations of enzyme (0, 10, 20, 50, 75, 100, and 200 nM), saturating AdoMet (30 μM), and saturating DNA (1 μM) in MRB supplemented with 0.2 mg/mL BSA in a total reaction volume of 70 μL. Reactions were initiated with addition of DNA. For the calf thymus initial velocity study, reaction mixtures contained 21 μM bp DNA so that it could be accurately compared with the 21 bp oligo. At specific time points that varied with enzyme concentration, the reaction in 10 μL of the mixture was quenched by submerging the mixture in 1% SDS. The resulting aliquots were spotted onto DE81 filter paper and processed as described above. Product formation versus time was plotted for each enzyme concentration in Sigma Plot. The corresponding slope for each curve is equal to the initial velocity at that enzyme concentration. Initial velocities were then plotted versus enzyme concentration, and the data were fit to a quadratic plot. To validate the quadratic nature of EcoDam, an enzyme-squared (E^2) replot analysis of the data was performed. If the reaction obeys second-order kinetics in relation to enzyme concentration, the E^2 replot should be linear.

Kinetic Modeling. Kinetic simulations to model EcoDam steady state data were performed using Scientist (MicroMath Scientific Software, Salt Lake City, UT) and Sigma Plot. Simultaneous global fitting analysis of steady state data with 2, 10, and 50 nM EcoDam were performed using the simplified reaction scheme illustrated in Figure 8. Goodness-of-fit statistics were used to evaluate the fit of the data to the reaction mechanism, yielding an R^2 value of 0.9815. Simulations derived from the global fit were plotted with the data as shown in Figure 8. Additionally, global fit analysis was performed with systematic removal of each kinetic branch with the exception of the Michaelis−Menten central branch.

RESULTS

Intrasite Processivity. EcoDam shows burst kinetics at 4 °C with the catalytic step ($k_{chem} = 2.88 \pm 0.36$ min^{-1}) preceding a much slower rate-determining step ($k_{cat} = 0.20 \pm 0.05$ min^{-1}), most likely product release. Single-turnover measurements with enzymes showing burst kinetics provide a direct measurement of the chemical step or any slower preceding steps. Our single-turnover reactions were conducted at 4 °C with limiting P DNA (400 nM) and a very slight excess of enzyme (420 nM) with saturating AdoMet (30 μM). We observed a total amount of

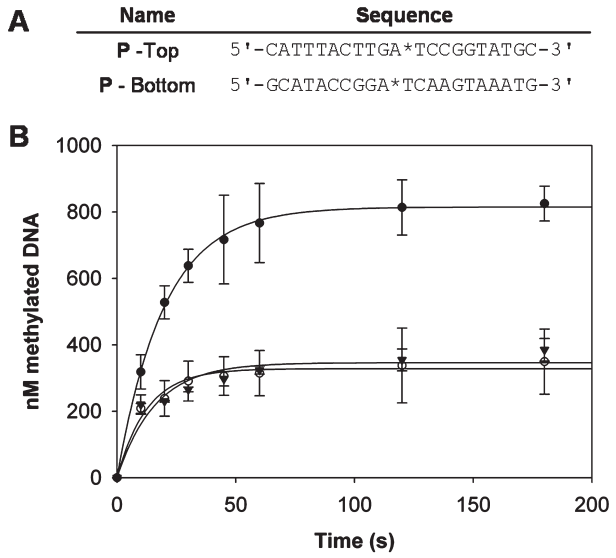

FIGURE 1: Single-turnover analysis of unmethylated and hemimethylated DNA reveals intrasite processivity by EcoDam. (A) Sequences for the DNA substrates. The preferred (P) substrate is the annealed product of the top and bottom strands shown. The asterisk indicates the position of the methylated adenine when hemimethylated substrates are used on either the top (HT) or bottom strand (HB). (B) Single-turnover assay with the preferred substrate when unmethylated (●), top-strand-hemimethylated (○), and bottom-strand-hemimethylated (▼). The DNA for each assay was limiting (400 nM), and EcoDam and AdoMet were in excess (420 nM and 30 μM, respectively). The asymptote for the single-exponential fit for the unmethylated preferred substrate is approximately equal to 2 times the actual DNA concentration in solution, indicating that both adenines in the palindromic GATC are methylated under these conditions. Conversely, the hemimethylated substrates asymptote at a concentration similar to the original DNA concentration added to the solution, meaning that only one adenine is methylated in a single-turnover event.

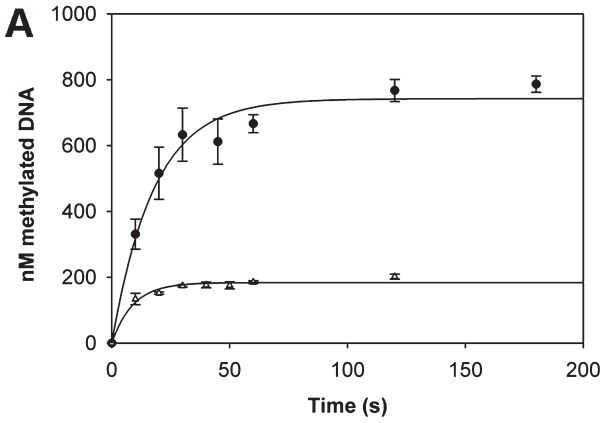

B

	M.HhaI	EcoDam
total product (nM)	183.7 +/- 5.3	742.1 +/- 26.2
input DNA (nM)	200	400

FIGURE 2: Single-turnover total product comparison reveals intrasite processivity by EcoDam and single methylation by M.HhaI on unmethylated cognate DNA. (A) Single-turnover reactions were conducted in MRB with excess enzyme and AdoMet. EcoDam reaction mixtures (●) contained 400 nM DNA and 420 nM enzyme, whereas M.HhaI reaction mixtures (○) contained 200 nM DNA and 220 nM enzyme due to variations in the K_D^{DNA} for each enzyme. (B) Comparison of the input DNA to the asymptote generated by the single-turnover assay for M.HhaI reveals one methylation event per turnover or an asymptote equal to the input DNA concentration. The asymptote for the EcoDam reaction is approximately double the input DNA concentration, suggesting that unmethylated GATC sites are methylated on both adenines within the limit of k_{cat}.

methylated DNA, or a *y*-asymptote, double the input unmethylated DNA concentration (Figure 1). The simplest explanation of our double methylation result is that two EcoDam molecules are able to bind the same unmethylated GATC site and modify both strands of the duplex within the confines of a single-turnover experiment as was previously observed with T4 Dam (*29*). However, our reaction conditions, unlike those used for T4 Dam where enzyme was in a large excess over DNA (~13:1), keep EcoDam in very slight excess over DNA (~1:1), making this scenario impossible. Therefore, our results suggest that two methyl transfer events occur per enzyme−substrate complex (intrasite processivity) since the rate constant for the methyl transfer (2.88 ± 0.35 min^{-1}) is significantly faster than that for product dissociation ($k_{cat} = 0.20 \pm 0.05$ min^{-1}) and the reaction time (3 min) is not sufficient for the enzyme to go through a k_{cat} step. Further, the resulting exponential curve derived from the single-turnover data fits to a single-exponential curve as opposed to a double exponential (observed with T4 Dam) that would result from two concerted steps. To verify our result, we tested the same DNA substrate (P) that was hemimethylated on the bottom strand or the top strand (Figure 1). Consistent with our results with unmethylated DNA, the total amount of methylated product generated in this case was exactly equal to the concentration of DNA that was used in the experiments. One would expect the total amount of methylated product to be approximately one-half the concentration of input DNA because of nonproductive binding events (*47*); however, this is not what we observed. Additionally, intrasite processive catalysis was further confirmed with a 21 bp duplex differing in nonspecific sequence but containing an unmethylated GATC site (data not shown).

We challenged EcoDam intrasite processivity further with a direct comparison with the well-characterized restriction modification methyltransferase M.HhaI. For EcoDam, we again observed intrasite processivity, or a total amount of methylated product approximately double the input DNA concentration signifying two methyl transfer events on unmethylated DNA (Figure 2). For the M.HhaI comparison, we employed unmethylated cognate DNA previously demonstrated to show single methylation events under single-turnover conditions (*48*). The single-turnover reaction for M.HhaI was conducted under conditions similar to those of the EcoDam reaction with enzyme (220 nM) in slight excess over DNA (200 nM) with saturating AdoMet (5 μM) in MRB (see Experimental Procedures). The overall concentrations of M.HhaI, cognate DNA, and AdoMet were decreased due to the relatively tight K_D^{DNA} and K_M^{SAM} values for M.HhaI, and the length of time of the assay was adjusted on the basis of the published k_{cat} for M.HhaI at 4 °C (*48*). Interestingly, the resulting total amount of methylated product for M.HhaI under single-turnover conditions was approximately equal to the input DNA concentration as previously reported for M.EcoRI, another type II DNA methyltransferase (*47*) (Figure 2). This side-by-side comparison allowed us to rule out the possibility of quenching factor errors entailed in the mathematical workup of the scintillation counts in addition to ruling out human error in the experiment itself.

Further support for intrasite processivity was sought using a burst magnitude approach. In a normal pre-steady state burst

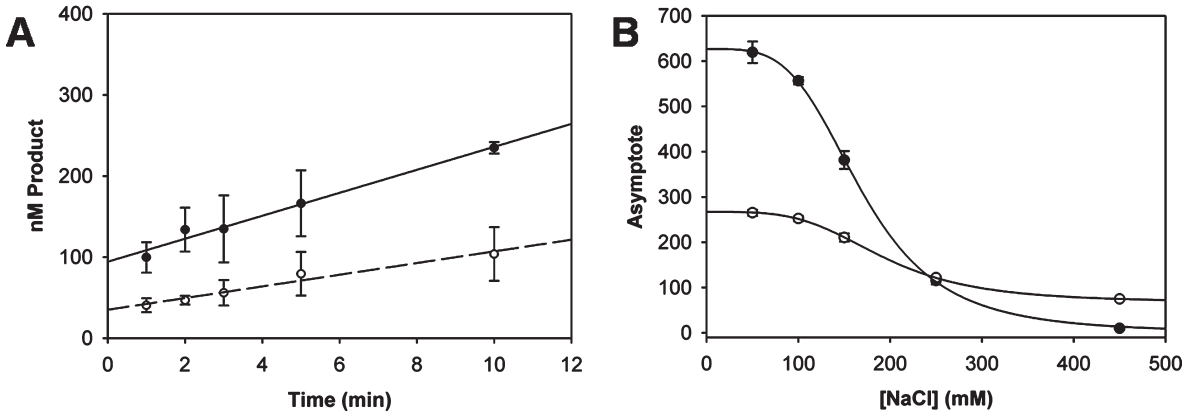

FIGURE 3: Burst analysis and salt dependence on double methylation suggest both strands are methylated prior to product release. (A) Pre-steady state burst analysis on unmethylated and hemimethylated preferred substrates at 4 °C. Reactions were performed with 50 nM EcoDam, 500 nM DNA, and saturating Sam in MRB. Reactions were quenched with equal volumes of 1% SDS at various time points and the results analyzed with Sigma Plot. Results were fit to a linear curve and the k_{cat}^{app} and burst magnitude derived from the slope and y-intercept of the best fit curve. (B) Single-turnover analysis of unmethylated P (●) and hemimethylated P HB (○) with increasing concentrations of salt. Reactions were conducted in MRB with 300 nM DNA and 320 nM EcoDam with saturating AdoMet. By measuring the extent of DNA methylation, these results reveal that double methylation events are highly dependent on the salt concentration of the solution. This indicates that continued association with the DNA is essential for double methylation to occur. Because of the effect of salt on K_D^{DNA}, P H-B was also tested to ensure that decreases in the concentration of total methylated DNA were not due to the enzyme's inability to bind DNA.

analysis, one would expect the burst magnitude, or extrapolated y-asymptote of the initial velocity curve, to be equal to or slightly less than the concentration of enzyme present in the reaction mixture (*47*). However, in a pre-steady state burst analysis with EcoDam on unmethylated P, we observe a burst magnitude double the input enzyme concentration (Figure 3A). These results suggest that two methyltransfers are occurring prior to the rate-determining step of product release or k_{cat}. This corroborates our single-turnover results and suggests that this phenomenon is not conditionally dependent on having an enzyme:DNA ratio of ~1 as the DNA concentration (500 nM) in pre-steady state analyses is in 10-fold molar excess in relation to the enzyme concentration (50 nM). Further confirmation was achieved when the same burst assay with hemimethylated DNA revealed a burst magnitude that was slightly lower than the input enzyme concentration as one would expect when the enzyme is saturated with substrate (Figure 3A). Burst reactions were conducted at 4 °C to verify the k_{cat}^{app} under these conditions which ensured proper timing for single-turnover assays, and to minimize temperature variability between the single-turnover and pre-steady state reactions.

Our previous results suggested that conserved phosphate interactions from the enzyme to the DNA backbone flanking the GATC site may be contributing to the processive nature of the enzyme (*43*). The crystal structure of EcoDam confirmed the position and interaction of the conserved residues with the DNA surrounding the cognate GATC site (*49*). Because of the processive nature of EcoDam and the conserved enzyme−DNA interface, we hypothesized that intrasite processivity could also be a result of the highly evolved ability of EcoDam to remain associated with the DNA, which might be expected to have a salt dependency distinct from that of the dissociation constant K_D^{DNA}. In other words, if EcoDam stays associated with the DNA following the first methyl transfer, then this association might have a distinct salt dependency when compared to that of the hemimethylated substrate. To test this, we determined the amount of methylated product under single-turnover conditions with increasing salt concentrations for both P and hemimethylated P DNA substrates. As seen in Figure 3B, the total amount of methylated product deriving from the unmethylated DNA sharply decreases with salt concentrations increasing from 50 to 150 mM NaCl in relation to the change that occurs with hemimethylated DNA in the same range. This suggests that intrasite processivity is dependent upon electrostatic interactions between EcoDam and the DNA phosphate backbone which may maintain the continued association of the enzyme with the DNA so that the second methylation occurs.

Dimerization. We used fluorescence anisotropy to determine the K_D^{DNA} for EcoDam in the presence of a saturating amount of the AdoMet analogue sinefungin. Reaction mixtures contained 10 nM DNA where one strand was labeled with a 5′-fluorescein. We observed a sigmoidal dependency on increasing enzyme concentration instead of the hyperbolic or near-hyperbolic association curve one would expect for a normal monomeric bound protein−DNA complex when titrating increasing amounts of EcoDam (Figure 4). Sigmoidal behavior associated with a Hill equation is typically observed with cooperative binding events and has been observed with other dimeric methyltransferases (*34*, *50*). We fit our data to both a modified quadratic equation and a Hill equation and found that the R^2 comparison between the two did, in fact, favor a Hill equation (Figure 4B). Further, the data yielded a Hill coefficient equal to 2.38 ± 0.17, suggesting positive cooperative binding between two EcoDam molecules. This result was confirmed with an additional 21 bp oligo duplex containing a GATC site to ensure this result was not an artifact of the P DNA sequence or composition used here (data not shown).

To test if dimerization can occur via two EcoDam molecules binding to the same DNA substrate, we performed a binding stoichiometry titration (Figure 5). In this reaction, DNA is at a concentration greater than the K_D^{DNA} and increasing amounts of EcoDam are added in the presence of a saturating level of sinefungin. Under these conditions, the amount of enzyme-bound DNA increases linearly until saturation is reached. The enzyme concentration at which the binding no longer increases divided by the concentration of substrate is equal to the ratio of enzyme bound per DNA molecule. In the case of EcoDam, linearity abruptly stops at ~1000 nM enzyme with 500 nM DNA present in solution (Figure 5). This corresponds to two EcoDam

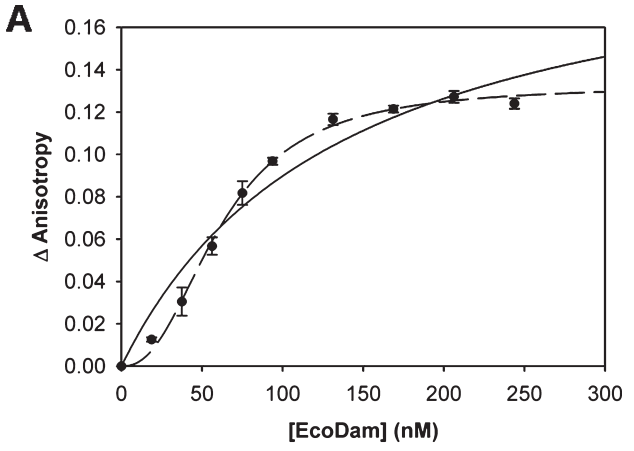

B

Quadratic		Hill Plot		
K_D^{DNA}	R^2	K_D^{DNA}	R^2	Coeff.
101.2 +/- 8.6	0.9527	61.7 +/- 2.0	0.9965	2.38 +/- .17

FIGURE 4: Fluorescence anisotropy on preferred and nonpreferred substrates reveals cooperative binding. (A) Fluorescence anisotropy was used to determine the binding affinity of EcoDam for the unmethylated preferred substrate. Reactions were performed with 20 nM fluorescein-labeled DNA and saturating sinefungin, while EcoDam was titrated into the solution at room temperature. Resultant changes in anisotropy were observed and plotted against enzyme concentration in Sigma Plot. Data were fit to the modified quadratic equation (—) and the Hill equation (– – –). (B) Comparison of the R^2 values between the modified quadratic equation and the Hill equation for P reveals a better fit for the Hill equation. The Hill coefficient is ~2, indicating that the cooperativity could be coming from two EcoDam molecules binding to the same GATC site. An additional anisotropy experiment performed on an independent 21 bp substrate also gave similar results (data not shown).

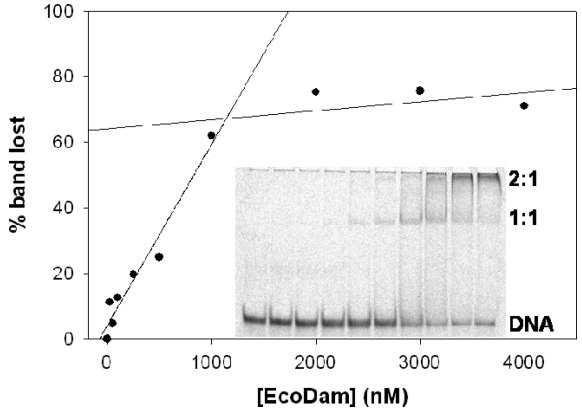

FIGURE 5: Two EcoDam molecules can bind to a single GATC-containing substrate. Binding stoichiometry reaction with P (500 nM), saturating sinefungin (50 μM), and increasing concentrations of EcoDam. The linear dependency on enzyme binding stops abruptly at an EcoDam concentration of 1000 nM, indicating that the binding stoichiometry of enzyme to substrate is 2:1. This result was verified with an additional 21 bp oligo nucleotide containing a GATC to confirm this result (data not shown).

molecules bound per DNA molecule or a 2:1 binding stoichiometry. We confirmed a 2:1 binding stoichiometry on a different 21 bp oligo containing an unmethylated GATC site to ensure that this result was not an artifact of the DNA sequence or composition (data not shown). The PAGE gel shown in Figure 5 reveals two different shifted bands: the first being what we perceive to be monomeric EcoDam binding to DNA and the second supershifted band corresponding to two EcoDam molecules per DNA molecule.

To determine if the substrate-dependent dimerization of EcoDam suggested by the anisotropy and stoichiometry experiments is functionally relevant, we conducted initial velocity studies using saturating amounts of P and hemimethylated P with various EcoDam concentrations. By monitoring the amount of methylated product versus time for each enzyme concentration, we were able to determine the initial velocity of each reaction (Figure 6A). As illustrated in Figure 6B, there is a quadratic relationship between initial velocity and enzyme concentration indicative of a higher-order protein−DNA complex that is more active than the lower-order form. This was the case for both unmethylated P and hemimethylated P. A replot of the squared concentration of the initial velocity data resulted in a linear curve, further validating the second-order dependency on enzyme concentration (Figure 6C). The classic interpretation of a quadratic relationship between enzyme and initial velocity is that monomeric enzyme exists at low concentrations of enzyme and is not as active as the dimeric form of the enzyme that dominates at the higher concentrations. This type of behavior has been observed with other methyltransferases that have been demonstrated to be dimeric, most notably with M.KpnI (*34*).

The most biologically relevant substrate for EcoDam is polymeric DNA containing multiple GATC sites. The processive nature of the enzyme ensures that EcoDam remains associated with the DNA in order to find multiple GATC sites to methylate prior to coming off of the substrate DNA (*22*). The ability of EcoDam to processively methylate multiple GATC sites is thought to increase the enzyme's efficient methylation of such substrates, thereby making possible the methylation of the ~20000 GATC sites in the *E. coli* genome (*5*, *22*). To test if the activity of the dimeric form of the enzyme could be observed on more biologically relevant DNA where EcoDam can behave processively, we used the initial velocity assay described above with calf thymus DNA (Figure 6D). The molarity, as defined in base pairs, is the same for calf thymus and the P substrate, which was saturating. The quadratic relationship between enzyme concentration and initial velocity observed on P is absent with calf thymus DNA (Figure 6D). The linear curve that fits to the calf thymus initial velocity plot is exactly what would be expected for a functional monomeric enzyme, meaning that the reaction is first-order in relation to enzyme concentration. This result is consistent with previous work that identified a monomeric EcoDam that hemimethylates plasmid and viral DNA (*22*, *51*). These data suggest that dimerization is substrate-dependent and more likely to occur on small single-site substrates as opposed to long, multisite substrates.

Substrate Activation. EcoDam steady state reactions were conducted with a large range of DNA concentrations (7.5−1000 nM). Although the enzyme appeared to obey standard Michaelis−Menten kinetics at the low concentrations of DNA typically used in these types of experiments with K_M^{DNA} and k_{cat} values similar to those previously published (*42*, *47*), higher DNA concentrations resulted in an activated form of the enzyme (Figure 7A). To ensure the legitimacy of the assay, a control reaction with M.HhaI and its cognate DNA resulted in k_{cat} and K_M^{DNA} values similar to those published (*48*) and revealed substrate inhibition when exposed to high concentrations of DNA (Figure 7A). Additionally, steady state reactions were

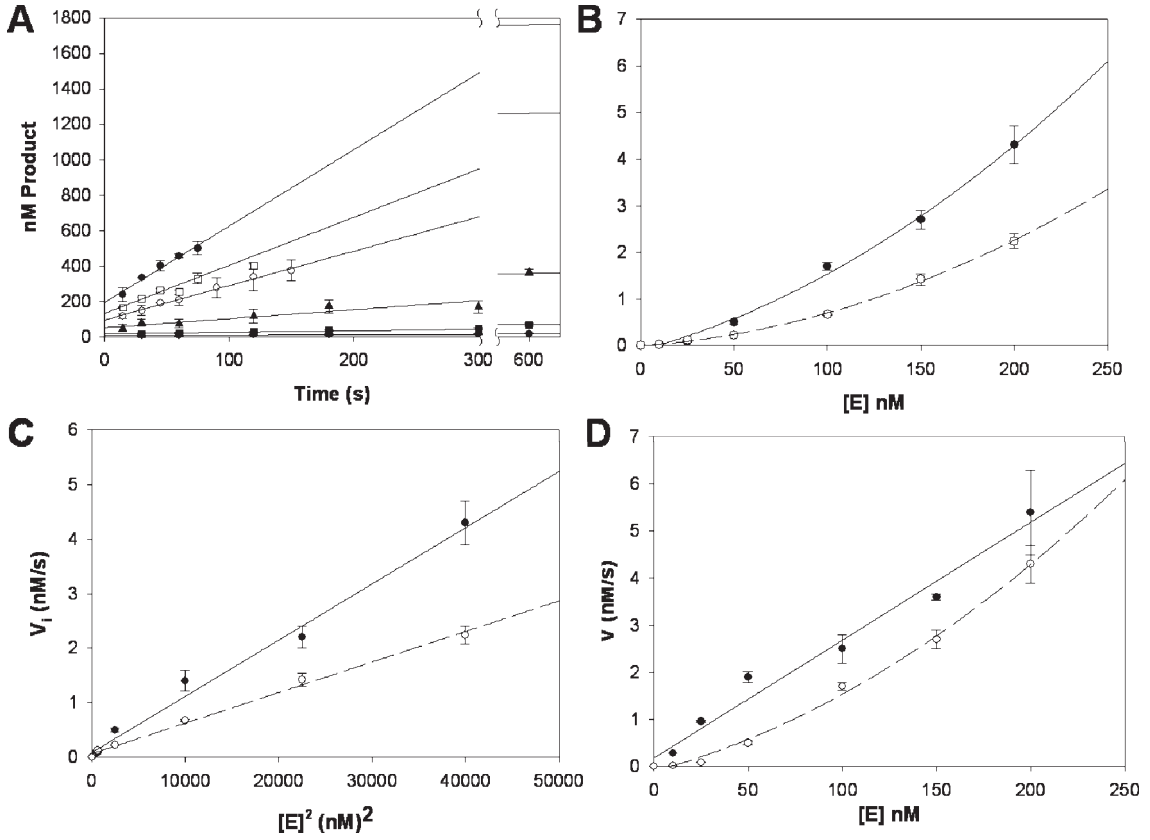

FIGURE 6: Initial velocity kinetics suggest EcoDam dimerization on P but not with calf thymus DNA. (A) Initial velocity studies with saturating DNA (1 μM) and Sam (30 μM) with increasing amounts of enzyme. Each reaction was fit to a linear curve in relation to product creation vs time. (B) The slope of the initial velocity curve or rate of product formation in relation to enzyme concentration reveals a quadratic relationship indicating a second-order dependency on enzyme concentration. This is true for both unmethylated (—) and hemimethylated (– – –) DNA. (C) The quadratic replot of initial velocity studies shows linearity when the squared concentration of enzyme is plotted vs initial velocity. This confirms the second-order dependency on enzyme concentration for both unmethylated (—) and hemimethylated (– – –) DNA. (D) Initial velocity studies with unmethylated P and calf thymus DNA. Linear behavior is observed with calf thymus DNA, indicating the methyl transfer reaction is not second-order in relation to enzyme concentration as is seen with P.

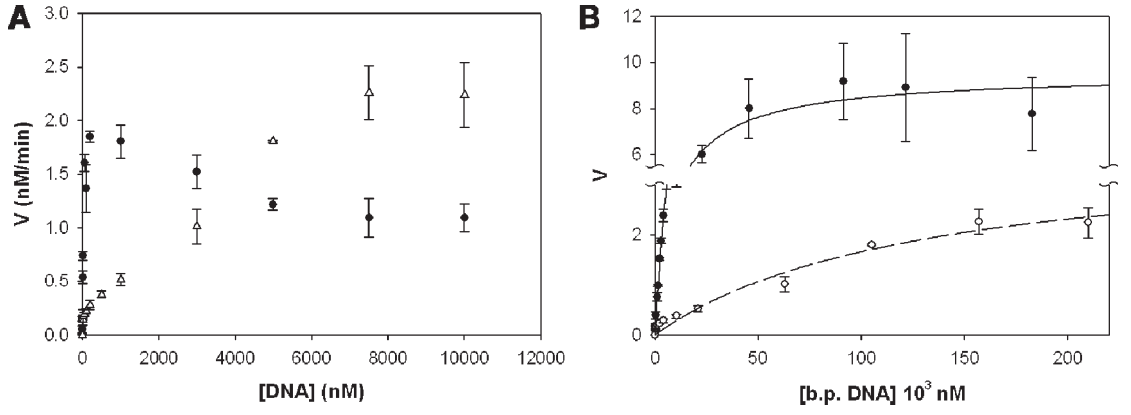

FIGURE 7: EcoDam shows activation by P substrate that is absent with calf thymus DNA. (A) Steady state reaction with EcoDam (△) and M. HhaI (●) on their respective cognate DNA oligos. Two saturation events occur with EcoDam; the first yields a $K_M{}^{DNA}$ and a k_{cat} that are similar to what has been previously published (10.6 ± 3.5 nM and 0.14 ± 0.01 min^{-1}, respectively). EcoDam reveals activation at high substrate concentrations, whereas M.HhaI shows substrate inhibition typically seen with DNA-modifying enzymes at such high concentrations of DNA. (B) Steady state V vs S plot of P substrate (○) and equal molar base pair concentrations of calf thymus DNA (●). Early data points reveal a primary saturation event with the P substrate that is not observed with the calf thymus substrate. Also, substrate activation is clearly apparent with P, whereas data of calf thymus DNA obey standard Michaelis–Menten kinetics and fit to a rectangular hyperbola.

conducted with calf thymus DNA with equimolar concentrations of base pairs as the 21 bp substrate (Figure 7B). This reaction yielded standard Michaelis–Menten kinetics with kinetic values similar to those observed on the activated form of the enzyme when exposed to high concentrations of small, synthetic substrate. Thus, the activation observed with high concentrations of 21 bp substrate is achieved even at low concentrations of calf thymus DNA.

Our initial velocity data suggest that there are two forms of active enzyme, presumably a monomeric form that dominates at low concentrations of enzyme and a dimeric form that dominates at high concentrations of enzyme (Figure 6). Therefore, as the

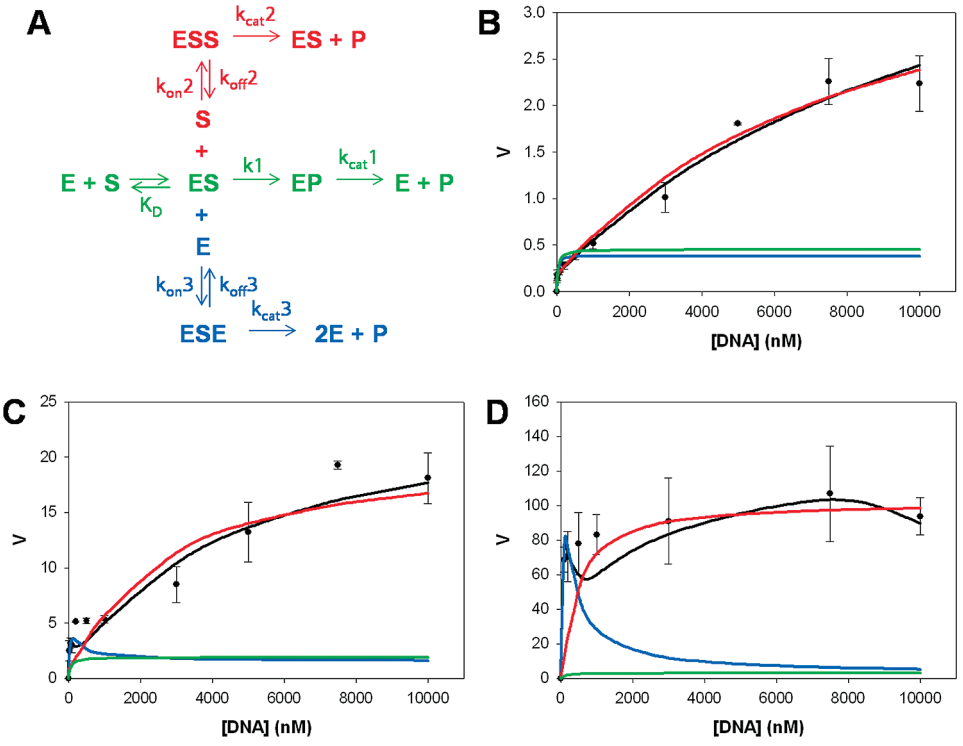

E

Parameter	Full Model	Dimerization	Substrate Activation	Michaelis-Menten
k1	1.59 +/- .36	0.30 +/- 0.15	19.32 +/- 45.07	0.91 +/- 0.45
K_D*	100*	100*	100*	100*
$k_{on}2$	0.77 +/- 45.29	0	3.63 +/- 347.57	0
$k_{off}2$	764 +/- 45421	0	220 +/- 21545	0
$k_{on}3$	0.59 +/- 0.11	0.14 +/- 0.05	0	0
$k_{off}3$#	0#	0#	0#	0#
$k_{cat}1$	0.10 +/- 0.01	0.88 +/- 1.18	0.09 +/- 0.01	0.32 +/- 0.13
$k_{cat}2$	2.45 +/- 0.24	0	2.04 +/- 0.32	0
$k_{cat}3$	7.45 +/- 1.43	155 +/- 1774	0	0
R^2	0.9815	0.7116	0.9073	0.5791
MSC	4.5065	1.8697	2.9687	1.5632

* = K_D value is fixed at 100 nM for all models (*See Results*)

= $k_{off}3$ is fixed at 0 for all models (*See Results*)

FIGURE 8: Kinetic modeling is consistent with dimerization and substrate activation of EcoDam. (A) The kinetic scheme used for the simultaneous global fitting analyses with the data shown in panels B−D is shown. Colors differentiate between various kinetic pathways (branches) where the full model (black), substrate activation branch (red), enzyme dimerization branch (blue), and standard Michaelis−Menten pathway (green) are shown. (B) Multiple global fitting analyses of steady state data with 2 nM enzyme. Reactions were performed by observing the amount of methylated product in the linear range of the reaction at a predetermined time point at various DNA concentrations. The data (●) fit excellently to the full model encompassing all kinetic pathways (black), whereas the relative fit and error increased when only the substrate activation model (red), dimerization (blue), or Michaelis−Menten pathway (green) was used to fit the data. Note that all models include the Michaelis−Menten branch. (C) Multiple global fitting analyses of the steady state data with 10 nM enzyme. (D) Multiple global fitting analyses of the steady state data with 50 nM enzyme. (E) Parameter and fitting results of the full, dimerization, substrate activation, and Michaelis−Menten models. Units are nanomolar and inverse minutes for all values.

concentration of enzyme increases, the dimeric form of the enzyme will also be predominant. We sought to determine kinetic parameters for both forms of the enzyme using steady state reaction conditions at multiple enzyme levels (2, 10, and 50 nM) whereby at 2 nM enzyme the monomeric form of the enzyme would be prevalent as opposed to 50 nM enzyme where the enzyme would be largely dimeric (Figure 8B−D). One would expect that the corresponding k_{cat} and K_M^{DNA} values derived from such assays would be representative of the population distribution of the forms of the enzyme at the concentrations probed. For example, at 2 nM enzyme the kinetic values would largely represent the monomer whereas at 50 nM enzyme the values would correspond to the dimer. At 10 nM enzyme a split population would be observed. Interestingly, at 10 nM enzyme two saturation events or two V_{max} asymptotes are apparent (Figure 8B). However, because of the complexity of the system (substrate activation and dimerization), we employed kinetic modeling to ensure that we were interpreting the data correctly.

Kinetic Modeling. The kinetic model shown in Figure 8 is for an enzyme that can both dimerize in the presence of substrate and

bind two substrate molecules as indicated by our results with small, synthetic DNA. Mathematical expressions corresponding to the three branched model are differentials in time which are integrated numerically. The initial proposed kinetic model contained 12 adjustable parameters containing on and off rates for all equilibrium events in addition to separate kinetic steps for the chemistry and product release steps for all branches. We were able to simplify this model to the scheme shown in Figure 8 due to the high correlation between some of the kinetic steps. The final model contained nine remaining adjustable parameters. Of these parameters, we fixed K_D equal to 100 nM as indicated by our own results described herein (Figure 4) as well as those previously published in the literature (*52*). Initial global fits between the data and model resulted in $k_{off}3$ approaching zero regardless of the initial values of each initial parameter; therefore, we fixed this value to zero. This modification did not affect the model selection criterion (see below), nor did it significantly impact the sum of the squared deviations as was anticipated. The remaining adjustable parameters were optimized by a simultaneous fit to all of the data shown in Figure 8; values of the parameters are given in Figure 8E. Similar results were obtained using different initial estimates.

The corresponding simulations derived from the optimized parameters are an excellent fit to the data for each enzyme concentration probed (Figure 8, black). To challenge this model to ensure that three branches are needed to satisfy the results obtained, we systematically removed each branch so that only substrate activation ($k_{cat}2$ pathway, Figure 8, red) or dimerization ($k_{cat}3$ pathway, Figure 8, blue) in conjunction with the standard Michaelis−Menten pathway exists. Constraints on the parameter values were kept constant in comparison with the three-branch pathway ($K_D = 100$ nM; $k_{off}3 = 0$); however, parameters involved in the removed pathway were set to zero. Additionally, fitting analysis was performed using only the central, Michaelis−Menten pathway ($k_{cat}1$, Figure 8, green). The simulations resulting from the removal of each pathway and the parameter values derived from each fit are shown for all enzyme concentrations in Figure 8.

As one can see in Figure 8E, the R^2 value for the fit of the full model is higher than that of any of the individual branches or combinations thereof. However, a better analysis of fit comes from the Model Selection Criterion (MSC) values of each model. The MSC is similar to the Akaike Information Criterion (AIC) commonly used in global fitting analyses. Both values represent the statistical goodness of fit and the number of parameters (degrees of freedom) that were required to obtain the fit. When comparing two models with different numbers of parameters, this criterion not only places a burden on the model with more parameters to have a better coefficient of determination but also quantifies how much better it must be for the model to be deemed more appropriate. The AIC is dependent on the magnitude of the data points as well as the number of observations, whereas the MSC will give the same rankings between models but has been normalized so that it is independent of the scaling of the data points. Therefore, the most appropriate model will be that with the largest MSC value (as opposed to the lowest AIC value). Figure 8E clearly shows that the largest MSC value corresponds to the three-branch model and drops off significantly when any branch is removed from the proposed kinetic scheme.

DISCUSSION

Processive catalysis occurs when an enzyme carries out multiple cycles of catalysis on the initially bound substrate rather than dissociating after the initial catalytic turnover (distributive catalysis) (*53*). Well-studied processive enzymes include the DNA and RNA polymerases that catalyze thousands of catalytic turnovers prior to substrate dissociation (*53*, *54*). Many DNA-modifying enzymes act processively. EcoDam, for example, differs from most restriction−modification methyltransferases due to the highly processive nature by which it methylates multiple GATC sites prior to dissociating from DNA (intersite processivity) (*22*). We recently demonstrated via site-directed mutagenesis that EcoDam processivity is modulated by conserved nonspecific phosphate interactions outside of the target GATC (*46*). These results suggest that EcoDam has evolved a unique mechanism to remain associated with DNA so that processive catalysis occurs. In this study, we further suggest that the highly evolved ability of EcoDam to remain associated with the DNA results in unique single-turnover and pre-steady state kinetics only partially mirrored by its ortholog T4 Dam. We found that, when limited to one turnover, EcoDam has the ability to methylate both strands of an unmethylated GATC site (Figure 1). This intrasite processive catalysis occurs prior to product release and is not observed with the nonprocessive restriction−modification methyltransferase M.HhaI (Figure 2).

It was previously suggested that EcoDam transfers one methyl group per DNA binding event (*21*). However, a weak coupling between the primary and secondary methyl transfer event was apparent when kinetic data were compared to computer simulations. The weak coupling was explained by assuming that EcoDam had a preference for hemimethylated GATC sites which was later shown not to be the case (*52*). For EcoDam to methylate both strands of an unmethylated GATC site prior to dissociation from the substrate, the enzyme must first orient itself productively onto the DNA for the initial methylation event, catalyze the methyl transfer, exchange AdoHcy for AdoMet, reorient itself productively onto the new hemimethylated site, and catalyze the second methyl transfer. Although this is seemingly improbable, other enzymes have been demonstrated to carry out intrasite processive catalysis. For example, AdoMet-dependent SET domain protein lysine methyltransferases carry out a similar if less ambitious rearrangement by reorienting a lysine in their active site two times to allow three methylation events prior to release of the modified histone (*55*). Further, T4 Dam has been shown to rapidly reorient itself on cognate GATC sites to increase methylation efficiency on small, synthetic substrates (*29*, *31*). Thus, there is suggestive literature precedence for kinetic behavior similar to EcoDam intrasite processivity.

The biological relevance of intrasite processive methylation of an unmethylated GATC site has particular importance when considering the epigenetically controlled *pap* regulon that produces the pilus proteins necessary for uropathogenic *E. coli* cellular adhesion (*38*). *pap* expression is dependent upon the methylation state of two GATC sites found within the regulon located proximal ($GATC^{prox}$) and distal ($GATC^{dist}$) to the gene (*56*, *57*). The transition of the fully methylated $GATC^{dist}$ and unmethylated $GATC^{prox}$ (phase off) to a fully methylated $GATC^{prox}$ and unmethylated $GATC^{dist}$ (phase on) is readily explained by intrasite processivity, without invoking two rounds of DNA replication prior to phase switching. However, it is unclear if intrasite processivity occurs on multisite substrates since the evidence presented here relies on the use of single-site substrates. The underlying mechanisms and regulation by multisite substrates are under investigation.

Many methyltransferases dimerize in solution, and some form functional dimers (*28*, *32*−*36*, *58*). For example, the orphan

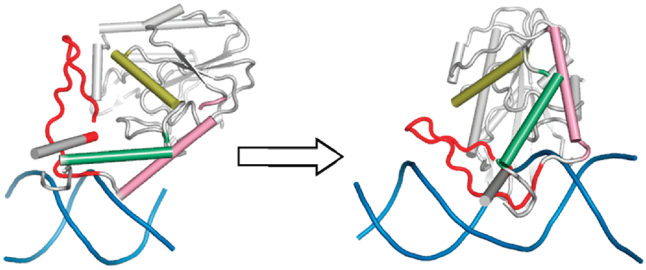

FIGURE 9: Transition from nonspecific to specific contacts from T4 Dam crystal structures. The nonspecific ternary structure of T4 Dam (Protein Data Bank entry 1YFL, left) shows the β-hairpin, and the loop regions surrounding it (red) are shown in a position perpendicular to the DNA helix (light blue). The β-hairpin contains residues involved in base-specific interactions within the target recognition domain. The ternary structure of T4 Dam bound to its cognate site (Protein Data Bank entry 1Q0T, right) shows the β-hairpin in a position parallel to the DNA helix to allow for base-specific contacts and intercalation necessary for the recognition of the GATC site. Select α-helices (yellow, green, and pink) are highlighted for observation of the protein movement upon the transition between nonspecific and specific DNA contacts.

methyltransferase CcrM dimerizes in solution at high concentrations but is only active as a monomer (*32*). M.KpnI was also shown to dimerize in solution; however, M.KpnI is more active in its dimeric state (*34*). Although both CcrM and KpnI belong to the β-class of N-6 methyltransferases, dimerization that results in an active or inactive enzyme has been observed in multiple classes of exocyclic amino methyltransferases in addition to the C-5 family containing M.HhaI (*28*). Importantly, dimerization has been observed in the α-class of methyltransferases which contains EcoDam, most notably with closely related ortholog T4 Dam (*31*).

Although EcoDam was shown to be monomeric in solution (*21*) and a functional monomer on polymeric DNA (*22*), we suggest that under certain conditions, EcoDam can behave as a substrate-dependent functional dimer. Similarly, T4 Dam was originally classified as a functional monomer but was later shown by gel filtration chromatography and chemical cross-linking to dimerize in the presence of small synthetic duplex DNA (*31*, *59*). These results are similar to the cooperative binding we observed with anisotropy (Figure 4) and a 2:1 EcoDam:DNA binding stoichiometry (Figure 5). The T4 dimer was found to be kinetically active under conditions where the level of enzyme was greater than the level of substrate (single-turnover conditions), catalyzing two methyltransfers per available GATC site on small, synthetic DNA (*29*, *59*). Again, this is not unlike our initial velocity results that suggest that at high EcoDam concentrations, a more active dimeric form of the enzyme is apparent (Figure 6). However, the reaction conditions used in the T4 Dam study contained a large excess of enzyme in relation to DNA (~13:1), leading the authors to conclude that two T4 Dam molecules were bound to a single DNA substrate, each catalyzing a unique methylation event (*59*). This hypothesis is consistent with the crystal structure of T4 Dam in which the enzyme crystallizes in a 2:1 enzyme:DNA ratio and two T4 Dam molecules are shown to bind to the same GATC site semispecifically via interactions with the DNA phosphate backbone (*60*). However, the single-turnover reaction conditions used in the T4 Dam study where the level of enzyme is much greater than the level of substrate leave open the possibility that the double-methylation event observed could have been due to intrasite processive catalysis, in which a monomeric enzyme executes two methylation cycles per binding event prior to becoming fully dissociated. Similar to T4 Dam, EcoDam also crystallized in a 2:1 enzyme:DNA ratio; however, two EcoDam molecules bound per GATC site was not observed (*49*). Although the 2:1 ratio was required for crystallization, each EcoDam molecule bound a unique GATC site located within the DNA substrate used or bridging DNA molecules that created an additional GATC site. Our single-turnover reaction conditions where the level of EcoDam is essentially equal to that of the DNA concentration (~1:1) make the "two-enzyme" scenario described for T4 Dam impossible (Figures 1 and 2). Further, when higher concentrations of EcoDam were introduced into the single-turnover reaction (~3:1), intrasite processivity was still observed (data not shown). Thus, the evidence for intrasite processive catalysis, involving two rounds of methylation on opposite DNA strands, is compelling as is a kinetically separate substrate-dependent dimerization event for EcoDam.

The ternary crystal structures available for T4 Dam offer insight into the nonspecific and specific interactions of enzymes in the α-class of methyltransferases (Figure 9) (*60*, *61*). Analysis of these structures provides plausible reaction intermediates for the conformational transitions between the enzyme methylating one strand and then translocating to methylate the other. As shown in Figure 9, the nonspecific complex of T4 Dam bound to DNA shows the β-hairpin positioned perpendicular to the DNA, which is reoriented to a position parallel to the DNA in the specific complex. The nonspecific complex offers a rare glimpse at what a nonspecific enzyme−DNA complex may look like while the enzyme is translocating for inter- or intrasite processivity. Further reorientation of the enzyme and positioning onto the DNA strand would result in another specific complex resulting in catalysis at that position. Additionally, the nonspecific T4 Dam structure in which two molecules are bound to the same GATC site could also offer evidence of the ability of two EcoDam molecules to be associated with the same GATC site as is observed in our binding and initial velocity assays (Figures 4−6).

We observe that EcoDam functions differently with large multisite DNA substrates (e.g., calf thymus) and short, synthetic duplexes (Figures 6D and 7B). Short duplexes are commonly used to study sequence-specific DNA-modifying enzymes because they offer many experimental advantages, including the ability to synthetically manipulate the cognate site, obtain exact concentrations of substrate, and use high concentrations of substrate to facilitate many reaction conditions. Our study suggests that the relevance of results obtained with one set of substrates (small duplexes) should be verified with the other (genomic DNA). However, we suggest that the in vivo situation may be a compromise between these very distinct substrate "environments". Although EcoDam is faced with highly polymeric DNA in which multiple GATC sites must be methylated, a particularly relevant consideration is that the majority of the bacterial genome is not readily accessible to EcoDam because of the high concentrations of numerous nonspecific DNA binding proteins (*38*, *62*, *63*). Thus, the actual in vivo circumstance may lie between the short single-site substrate and the highly accessible, large and multisite substrates. It is not surprising then that EcoDam may have evolved a unique mechanism (intrasite processivity) for dealing with the situation in which it can no longer traverse linearly along DNA (intersite processivity). Certainly, our results suggest that EcoDam has the inherent ability to respond to the nature of the DNA to which it is bound (long or short) by becoming activated by substrate or enzyme−enzyme

interactions. Regardless, our results suggest that studies with small, synthetic duplexes should be complemented by studies with more biologically relevant DNA to gain a better understanding of how an enzyme works in two-dimensional and three-dimensional space.

ACKNOWLEDGMENT

We thank Dr. Dan Morse and his research group for the use of their fluorimeter for anisotropy experiments. We also thank Dr. Stan Parsons for his guidance through kinetic modeling.

REFERENCES

1. Bestor, T. H., and Verdine, G. L. (1994) DNA Methyltransferases. *Curr. Opin. Cell Biol. 6*, 380–389.
2. Cheng, X. D., and Roberts, R. J. (2001) AdoMet-dependent methylation, DNA methyltransferases and base flipping. *Nucleic Acids Res. 29*, 3784–3795.
3. Cheng, X. D. (1995) Structure and Function of DNA Methyltransferases. *Annu. Rev. Biophys. Biomol. Struct. 24*, 293–318.
4. Wilson, G. G. (1991) Organization of Restriction-Modification Systems. *Nucleic Acids Res. 19*, 2539–2566.
5. Casadesus, J., and Low, D. (2006) Epigenetic gene regulation in the bacterial world. *Microbiol. Mol. Biol. Rev. 70*, 830–856.
6. Lobner-Olesen, A., Skovgaard, O., and Marinus, M. G. (2005) Dam methylation: Coordinating cellular processes. *Curr. Opin. Microbiol. 8*, 154–160.
7. Low, D. A., and Casadesus, J. (2008) Clocks and switches: Bacterial gene regulation by DNA adenine methylation. *Curr. Opin. Microbiol. 11*, 106–112.
8. Wion, D., and Casadesus, J. (2006) N-6-Methyl-adenine: An epigenetic signal for DNA-protein interactions. *Nat. Rev. Microbiol. 4*, 183–192.
9. Wright, R., Stephens, C., and Shapiro, L. (1997) The CcrM DNA methyltransferase is widespread in the α subdivision of proteobacteria, and its essential functions are conserved in *Rhizobium meliloti* and *Caulobacter crescentus*. *J. Bacteriol. 179*, 5869–5877.
10. Heithoff, D. M., Sinsheimer, R. L., Low, D. A., and Mahan, M. J. (1999) An essential role for DNA adenine methylation in bacterial virulence. *Science 284*, 967–970.
11. Julio, S. M., Heithoff, D. M., Provenzano, D., Klose, K. E., Sinsheimer, R. L., Low, D. A., and Mahan, M. J. (2001) DNA adenine methylase is essential for viability and plays a role in the pathogenesis of *Yersinia pseudotuberculosis* and *Vibrio cholerae*. *Infect. Immun. 69*, 7610–7615.
12. Eberhard, J., Oza, J., and Reich, N. O. (2001) Cloning, sequence analysis and heterlogous expression of the DNA adenine-(N-6) methyltransferase from the human pathogen *Actinobacillus actinomycetemcomitans*. *FEMS Microbiol. Lett. 195*, 223–229.
13. Piekarowicz, A., Brzezinski, R., and Kauc, L. (1975) Host Specificity of DNA in *Hemophilus influenzae*: In vivo Action of Restriction Endonucleases on Phage and Bacterial DNA. *Acta Microbiol. Pol., Ser. A 7*, 51–65.
14. Heusipp, G., Falker, S., and Schmidt, M. A. (2007) DNA adenine methylation and bacterial pathogenesis. *Int. J. Med. Microbiol. 297*, 1–7.
15. Alonso, A., Pucciarelli, M. G., Figueroa-Bossi, N., and Garcia-del Portillo, F. (2005) Increased excision of the *Salmonella* prophage ST64B caused by a deficiency in dam methylase. *J. Bacteriol. 187*, 7901–7911.
16. Oshima, T., Wada, C., Kawagoe, Y., Ara, T., Maeda, M., Masuda, Y., Hiraga, S., and Mori, H. (2002) Genome-wide analysis of deoxyadenosine methyltransferase-mediated control of gene expression in *Escherichia coli*. *Mol. Microbiol. 45*, 673–695.
17. Watson, M. E., Jarisch, J., and Smith, A. L. (2004) Inactivation of deoxyadenosine methyltransferase (dam) attenuates *Haemphilus influenzae* virulence. *Mol. Microbiol. 53*, 651–664.
18. Wu, H., Lippmann, J. E., Oza, J. P., Zeng, M., Fives-Taylor, P., and Reich, N. O. (2006) Induced Mutagenesis in Dam[-]Mutants of *Escherichia coli*: Role for 6-Methyladenine Residues in Mutation Avoidance. *Oral Microbiol. Immunol. 21*, 238–244.
19. Andersson, D. I. (2003) Persistence of antibiotic resistant bacteria. *Curr. Opin. Microbiol. 6*, 452–456.
20. Mashhoon, N., Pruss, C., Carroll, M., Johnson, P. H., and Reich, N. O. (2006) Selective inhibitors of bacterial DNA adenine methyltransferases. *J. Biomol. Screening 11*, 497–510.
21. Herman, G. E., and Modrich, P. (1982) *Escherichia coli* Dam Methylase: Physical and Catalytic Properties of the Homogeneous Enzyme. *J. Biol. Chem. 257*, 2605–2612.
22. Urig, S., Gowher, H., Hermann, A., Beck, C., Fatemi, M., Humeny, A., and Jeltsch, A. (2002) The *Escherichia coli* dam DNA methyltransferase modifies DNA in a highly processive reaction. *J. Mol. Biol. 319*, 1085–1096.
23. Boye, E., Marinus, M. G., and Lobnerolesen, A. (1992) Quantitation of Dam Methyltransferase in *Escherichia coli*. *J. Bacteriol. 174*, 1682–1685.
24. Szyf, M., Avrahamhaetzni, K., Reifman, A., Shlomai, J., Kaplan, F., Oppenheim, A., and Razin, A. (1984) DNA Methylation Pattern is Determined by the Intracellular Level of the Methylase. *Proc. Natl. Acad. Sci. U.S.A. 81*, 3278–3282.
25. Glickman, B., Vandenelsen, P., and Radman, M. (1978) Induced Mutagenesis in Dam[-]Mutants of *Escherichia coli*: Role for 6-Methyladenine Residues in Mutation Avoidance. *Mol. Gen. Genet. 163*, 307–312.
26. Herman, G. E., and Modrich, P. (1981) *Escherichia coli* K-12 Clones that Overproduce Dam Methylase are Hypermutable. *J. Bacteriol. 145*, 644–646.
27. Modrich, P. (1991) Mechanisms and Biological Effects of Mismatch Repair. *Annu. Rev. Genet. 25*, 229–253.
28. Dong, A. P., Zhou, L., Zhang, X., Stickel, S., Roberts, R. J., and Cheng, X. D. (2004) Structure of the Q237W mutant of HhaI DNA methyltransferase: An insight into protein-protein interactions. *Biol. Chem. 385*, 373–379.
29. Malygin, E. G., Lindstrom, W. M., Zinoviev, V. V., Evdokimov, A. A., Schlagman, S. L., Reich, N. O., and Hattman, S. (2003) Bacteriophage T4 Dam (DNA-(adenine-N-6)-methyltransferase): Evidence for two distinct stages of methylation under single turnover conditions. *J. Biol. Chem. 278*, 41749–41755.
30. De La Campa, A. G., Kale, P., Springhorn, S. S., and Lacks, S. A. (1987) Proteins Encoded by the DpnII Restriction Gene Cassette. *J. Mol. Biol. 196*, 457–469.
31. Zinoviev, V. V., Evdokimov, A. A., Hattman, S., and Malygin, E. G. (2004) Molecular enzymology of phage T4 Dam DNA methyltransferase. *Mol. Biol. 38*, 737–751.
32. Shier, V. K., Hancey, C. J., and Benkovic, S. J. (2001) Identification of the active oligomeric state of an essential adenine DNA methyltransferase from *Caulobacter crescentus*. *J. Biol. Chem. 276*, 14744–14751.
33. Mruk, L., Cichowicz, M., and Kaczorowski, T. (2003) Characterization of the LlaCI methyltransferase from *Lactococcus lactis* subsp *cremoris* W15 provides new insights into the biology of type II restriction-modification systems. *Microbiology* (*Reading, U.K.*) *149*, 3331–3341.
34. Bheemanaik, S., Chandrashekaran, S., Nagaraja, V., and Rao, D. N. (2003) Kinetic and catalytic properties of dimeric KpnI DNA methyltransferase. *J. Biol. Chem. 278*, 7863–7874.
35. Osipiuk, J., Walsh, M. A., and Joachimiak, A. (2003) Crystal structure of MboIIA methyltransferase. *Nucleic Acids Res. 31*, 5440–5448.
36. Scavetta, R., Thomas, C. B., Walsh, M. A., Szegedi, S., Joachimiak, A., Gumport, R. I., and Churchill, M. E. A. (2000) Structure of RsrI methyltransferase, a member of the N6-adenine β class of DNA methyltransferases. *Nucleic Acids Res. 28*, 3950–3961.
37. Franke, I., Meiss, G., and Pingoud, A. (1999) On the advantage of being a dimer, a case study using the dimeric *Serratia* nuclease and the monomeric nuclease from *Anabaena* sp. Strain PCC 71209. *J. Biol. Chem. 274*, 825–832.
38. Peterson, S. N., and Reich, N. O. (2008) Competitive Lrp and Dam Assembly at the pap Regulatory Region: Implications for Mechanisms of Epigenetic Regulation. *J. Mol. Biol. 383*, 92–105.
39. Waldron, D. E., Owen, P., and Dorman, C. J. (2002) Competitive interaction of the OxyR DNA-binding protein and the Dam methylase at the antigen 43 gene regulatory region in *Escherichia coli*. *Mol. Microbiol. 44*, 509–520.
40. Tavazoie, S., and Church, G. M. (1998) Quantitative whole-genome analysis of DNA-protein interactions by in vivo methylase protection in *E. coli*. *Nat. Biotechnol. 16*, 566–571.
41. Wang, M. X., and Church, G. M. (1992) A Whole Genome Approach to In vivo DNA-Protein Interactions in *Escherichia coli*. *Nature 360*, 606–610.
42. Coffin, S. R., and Reich, N. O. (2008) Modulation of *Escherichia coli* DNA methyltransferase activity by biologically derived GATC-flanking sequences. *J. Biol. Chem. 283*, 20106–20116.
43. Peterson, S. N., and Reich, N. O. (2006) GATC flanking sequences regulate dam activity: Evidence for how Dam specificity may influence pap expression. *J. Mol. Biol. 355*, 459–472.

44. Bergerat, A., Guschlbauer, W., and Fazakerley, G. V. (1991) Allosteric and Catalytic Binding of S-Adenosylmethionine to *Escherichia coli* DNA Adenine Methyltransferase Monitored by ^{3}H NMR. *Proc. Natl. Acad. Sci. U.S.A. 88*, 6394–6397.
45. Liebert, K., Horton, J. R., Chahar, S., Orwick, M., Cheng, X. D., and Jeltsch, A. (2007) Two alternative conformations of S-Adenosyl-L-Homocysteine bound to *Escherichia coli* DNA adenine methyltransferase and the implication of conformational changes in regulating the catalytic cycle. *J. Biol. Chem. 282*, 22848–22855.
46. Coffin, S. R., and Reich, N. (2009) *Escherichia coli* DNA Adenine Methyltransferase: The Structural Basis of Processive Catalysis and Indirect Read-Out. *J. Biol. Chem. 284*, 18390–18400.
47. Reich, N. O., and Mashhoon, N. (1993) Presteady State Kinetics of an S-Adenosylmethionine-Dependent Enzyme: Evidence for a Unique Binding Orientation Requirement for EcoRI DNA Methyltransferase. *J. Biol. Chem. 268*, 9191–9193.
48. Estabrook, R. A., and Reich, N. (2006) Observing an induced-fit mechanism during sequence-specific DNA methylation. *J. Biol. Chem. 281*, 37205–37214.
49. Horton, J. R., Liebert, K., Bekes, M., Jeltsch, A., and Cheng, X. D. (2006) Structure and substrate recognition of the *Escherichia coli* DNA adenine methyltransferase. *J. Mol. Biol. 358*, 559–570.
50. Thomas, C. B., and Gumport, R. I. (2006) Dimerization of the bacterial RsrI N6-adenine DNA methyltransferase. *Nucleic Acids Res. 34*, 806–815.
51. Bergerat, A., Kriebardis, A., and Guschlbauer, W. (1989) Preferential Site-Specific Hemimethylation of GATC Sites in pBR322 DNA by Dam Methyltransferase from *Escherichia coli*. *J. Biol. Chem. 264*, 4064–4070.
52. Mashhoon, N., Carroll, M., Pruss, C., Eberhard, J., Ishikawa, S., Estabrook, R. A., and Reich, N. (2004) Functional characterization of *Escherichia coli* DNA adenine methyltransferase, a novel target for antibiotics. *J. Biol. Chem. 279*, 52075–52081.
53. VonHippel, P. H., Fairfield, F. R., and Dolejsi, M. K. (1994) On the Processivity of Polymerases. *DNA Damage 726*, 118–131.
54. Breyer, W. A., and Matthews, B. W. (2001) A Structural Basis for Processivity. *Protein Sci. 10*, 1699–1711.
55. Qian, C., and Zhou, M. M. (2006) SET domain protein lysine methyltransferases: Structure, specificity and catalysis. *Cell. Mol. Life Sci. 63*, 2755–2763.
56. Hernday, A., Krabbe, M., Braaten, B., and Low, D. (2002) Self-perpetuating epigenetic pili switches in bacteria. *Proc. Natl. Acad. Sci. U.S.A. 99*, 16470–16476.
57. Hernday, A. D., Braaten, B. A., and Low, D. A. (2003) The mechanism by which DNA adenine methylase and papI activate the pap epigenetic switch. *Mol. Cell 12*, 947–957.
58. Bheemanaik, S., Reddy, Y. V. R., and Rao, D. N. (2006) Structure, function, and mechanism of exocyclic DNA methyltransferases. *Biochem. J. 399*, 177–190.
59. Malygin, E. G., Ovechkina, L. G., Evdokimov, A. A., and Zinoviev, V. V. (2001) Single turnover kinetics of methylation by T4 DNA-(N6-adenine)-methyltransferase. *Mol. Biol. 35*, 56–68.
60. Yang, Z., Horton, J. R., Zhou, L., Zhang, X. J., Dong, A. P., Zhang, X., Schlagman, S. L., Kossykh, V., Hattman, S., and Cheng, X. D. (2003) Structure of the bacteriophage T4 DNA adenine methyltransferase. *Nat. Struct. Biol. 10*, 849–855.
61. Horton, J. R., Liebert, K., Hattman, S., Jeltsch, A., and Cheng, X. D. (2005) Transition from nonspecific to specific DNA interactions along the substrate-recognition pathway of Dam methyltransferase. *Cell 121*, 349–361.
62. Peterson, S. N., Dahlquist, F. W., and Reich, N. O. (2007) The role of high affinity non-specific DNA binding by Lrp in transcriptional regulation and DNA organization. *J. Mol. Biol. 369*, 1307–1317.
63. Thanbichler, M., Wang, S. C., and Shapiro, L. (2005) The bacterial nucleoid: A highly organized and dynamic structure. *J. Cell. Biochem. 96*, 506–521.